

# Reactions of Peptides with Class II Proteins of the Major Histocompatibility Complex

Craig Beeson and Harden M. McConnell\*

Contribution from the Department of Chemistry, Stanford University, Stanford, California 94305

Received April 25, 1995<sup>®</sup>

**Abstract:** The kinetics of the reactions of peptides with class II proteins of the major histocompatibility complex (MHC) are simulated so as to include the spontaneous inactivation of peptide-free MHC proteins. These simulations include the kinetics of loss of endogenous peptides normally present in preparations of these proteins and, in some cases, the formation of kinetic intermediates in the binding of added peptides to peptide-free proteins. In these reactions the amount of complex between the MHC protein and added peptide does not represent an equilibrium state of the system but rather a quasistationary concentration that is the result of a competition between peptide binding and inactivation of the peptide-free protein. It is shown that in spite of these complex kinetics, Scatchard plots of simulated binding data are frequently linear, as observed experimentally. However, the “equilibrium constants” derived from the slopes of such plots bear no simple relationship to the true equilibrium constants for the reactions.

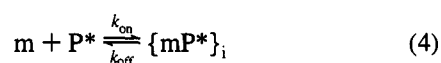
## Introduction

The triggering of T cells by peptides bound to the class II proteins of the major histocompatibility complex (MHC) is a critical event in the generation of an immune response<sup>1</sup> and selection of the lymphocyte repertoire.<sup>2</sup> One step in this process, the formation of MHC protein–peptide complexes, has been the focus of a number of studies.<sup>3–9</sup> These complexes are interesting in that the proteins involved have the capacity to bind hundreds of different peptides, often with long dissociation lifetimes, on the order of hours to days.<sup>10</sup> The broad selectivity and high kinetic stability is partly explained by a recent crystal structure of an MHC protein–peptide complex. Binding is stabilized by an array of hydrogen bonds between protein side chains and the peptide amide backbone.<sup>11</sup> The involvement of multiple binding interactions in the reactions of peptides and MHC proteins yields complex reaction kinetics.<sup>4–8</sup> Thus, the kinetics of the formation and dissociation of MHC protein–peptide complexes are of interest from the point of view of protein folding, as well as immunological function.<sup>12</sup>

A number of kinetic studies of MHC protein–peptide reactions can be understood in terms of kinetic eqs 1–3.<sup>3–9</sup>



Reaction 1 describes the dissociation of peptides ( $P_e$ , endogenous or “self” peptides) that are often present in preparations of purified samples of this protein.<sup>10</sup> The rates of binding for added labeled peptide ( $P^*$ ) are relatively insensitive to  $P^*$  concentrations, since binding reaction 2 is limited by dissociation reaction 1.<sup>8</sup> Recent work has shown that peptide-free MHC protein undergoes an inactivation reaction 3 at 37 °C.<sup>4–7,13</sup> The presence of endogenous peptides together with the inactivation reaction has led to substantial uncertainty concerning the equilibrium constants for these reactions. The kinetic analyses are also sometimes complicated by the role of kinetic intermediates, described by the reactions 4 and 5.<sup>4b,5</sup>



The complex reactions described by eqs 1–5 are not apparent in equilibrium binding analyses of MHC protein–peptide reactions. The simulations given in the present paper were stimulated by a desire to understand why the reported Scatchard plots for many of these reactions are nearly linear and correspond to micromolar equilibrium constants.<sup>3a</sup> It is demon-

(12) Sadegh-Nasseri, S.; Germain, R. N. *Immunol. Today* 1992, 13, 43–46.

(13) The nature of the inactivation reaction is not known. Dissociation of the murine MHC protein I-E<sup>k</sup> heterodimer into single chains has been observed in octyl glucoside solutions.<sup>6</sup> However, the related I-E<sup>d</sup> protein undergoes the inactivation reaction in dodecyl maltoside solutions even though it is stable to heterodimer cleavage under these conditions.<sup>5</sup> Inactivation has also been observed for the human MHC protein DR1 in detergent free solutions.<sup>4b</sup>

<sup>®</sup> Abstract published in *Advance ACS Abstracts*, October 15, 1995.

(1) Jorgensen, J. L.; Reay, P. A.; Ehrlich, E. W.; Davis, M. M. *Annu. Rev. Immunol.* 1992, 10, 835–873. Germain, R. N.; Margulies, D. H. *Annu. Rev. Immunol.* 1993, 11, 403–450.

(2) Allen, P. M. *Cell* 1994, 76, 593–596.

(3) (a) Rothbard, J. B.; Gefter, M. L. *Annu. Rev. Immunol.* 1991, 9, 527–565. (b) Witt, S. N.; McConnell, H. M. *Acc. Chem. Res.* 1993, 26, 442–448.

(4) (a) Sadegh-Nasseri, S.; McConnell, H. M. *Nature (London)* 1989, 337, 274–276. (b) Sadegh-Nasseri, S.; Stern, L. J.; Wiley, D. C.; Germain, R. N. *Nature (London)* 1994, 370, 647–650.

(5) Beeson, C.; McConnell, H. M. *Proc. Natl. Acad. Sci. U.S.A.* 1994, 91, 8842–8845.

(6) Witt, S. N.; McConnell, H. M. *J. Am. Chem. Soc.* 1992, 114, 3506–3511.

(7) Mason, K.; McConnell, H. M. *Proc. Natl. Acad. Sci. U.S.A.* 1994, 91, 12463–12466. Mason, K.; Denney, D. W., Jr.; McConnell, H. M. *J. Immunol.* 1995, 154, 5216–5227.

(8) Tampe, R.; McConnell, H. M. *Proc. Natl. Acad. Sci. U.S.A.* 1991, 88, 4661–4665. Witt, S. N.; McConnell, H. M. *Proc. Natl. Acad. Sci. U.S.A.* 1991, 88, 8164–8168.

(9) Stern, L. J.; Wiley, D. C. *Cell* 1992, 68, 465–477.

(10) Rudensky, A. Y.; Preston-Hurlbert, P.; Al-Ramadi, B. K.; Rothbard, J.; Janeway, C. A. *J. Nature (London)* 1992, 359, 429–431. Chicz, R. M.; Urban, R. G.; Gorga, J. C.; Vignali, A. A.; Lane, W. S.; Strominger, J. L. *J. Exp. Med.* 1993, 178, 27–47.

(11) Stern, L. J.; Brown, J. H.; Jardetzky, T. S.; Gorga, J. C.; Urban, R. G.; Strominger, J. L.; Wiley, D. C. *Nature (London)* 1994, 368, 215–221.

strated that, despite the complex kinetics, Scatchard plots for these reactions are frequently linear. Not surprisingly, the slopes of the Scatchard plots are not simply related to the equilibrium constants. It is suggested that equilibrium constants reported for peptides binding to MHC proteins must be interpreted with caution. More generally, these results demonstrate the potential pitfall associated with the application of equilibrium models to receptor–ligand reactions that yield superficially linear Scatchard plots.

### Experimental Section

**Kinetic Rate Constants.** Kinetic rate constants for the reactions between peptides and four different murine class II MHC proteins (I-A<sup>d</sup>, I-A<sup>k</sup>, I-E<sup>d</sup>, and I-E<sup>k</sup>) were taken from the literature.<sup>3–9</sup> Kinetic rate constants for the reactions between peptides and a human class II MHC protein (DR1) were estimated from ref 3b. Experimental data for the binding of the myelin basic protein Ac(1–14)A<sup>d</sup> peptide were taken from ref 7. Experimental data for the reactions of the hen egg white lysozyme 46–61 peptide with the MHC protein (I-A<sup>k</sup>) were obtained as described in ref 5. Briefly, the lysozyme peptide was labeled at the N-terminus with carboxyfluorescein<sup>7</sup> and incubated with the MHC protein in dodecyl maltoside at 37 °C. Association of the peptide with the MHC protein was measured by high performance size exclusion chromatography with a fluorescence detector.<sup>5</sup> Estimates for  $k_e$  were obtained from a double exponential function fit to the binding data.

**Mechanism Simulations.** Two mechanisms for the reactions of peptides with MHC proteins were simulated. The simplest mechanism, eqs 1–3, is described by the differential eqs 6–9. The rebinding of endogenous peptide, the reverse of eq 1, has been neglected (see below).

$$d[mP_e(t)]/dt = -d[P_e(t)]/dt = -k_e[mP_e(t)] \quad (6)$$

$$d[m(t)]/dt = k_e[mP_e(t)] + k_{off}[mP^*(t)] - k_{on}[m(t)P^*(t)] - k_i[m(t)] \quad (7)$$

$$d[mP^*(t)]/dt = -d[P^*(t)]/dt = k_{on}[m(t)P^*(t)] - k_{off}[mP^*(t)] \quad (8)$$

$$d[\underline{m}(t)]/dt = k_i[m(t)] \quad (9)$$

A more complete mechanism in which eq 2 is replaced by eqs 4 and 5 is described by the differential eqs 10–14.

$$d[mP_e(t)]/dt = d[P_e(t)]/dt = -k_e[mP_e(t)] \quad (10)$$

$$d[m(t)]/dt = k_e[mP_e(t)] + k_{off}[\{mP^*\}_i(t)] - k_{on}[m(t)P^*(t)] - k_i[m(t)] \quad (11)$$

$$d[\{mP^*\}_i(t)]/dt = -d[P^*(t)]/dt = k_{on}[m(t)P^*(t)] - (k_{off} + k_r)[\{mP^*\}_i(t)] + k_r[mP^*(t)] \quad (12)$$

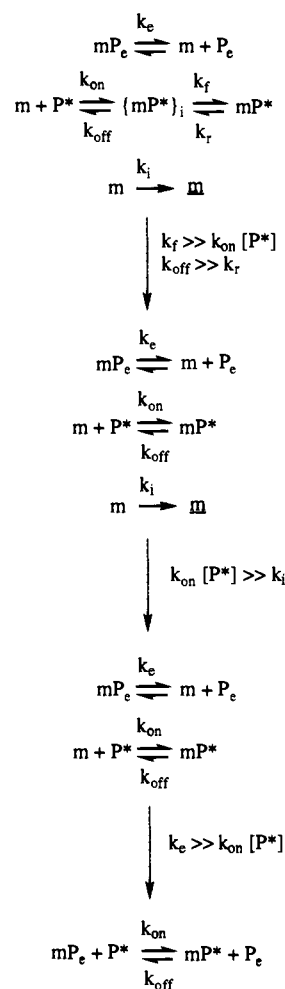
$$d[mP^*(t)]/dt = k_r[\{mP^*\}_i(t)] - k_i[mP^*(t)] \quad (13)$$

$$d[\underline{m}(t)]/dt = k_i[m(t)] \quad (14)$$

The coupled differential eqs 6–9 and 10–14 were solved numerically with Mathematica V. 2.2 (Wolfram Research, IL) using the default step sizes, precision, and accuracy goals. The dissociation rate constants ( $k_e$ ,  $k_{off}$ ) were 3–0.001 h<sup>-1</sup>, which encompass the range of reported values.<sup>3–9</sup> The association rate constants ( $k_{on}$ ) ranged from 0.36 to 36 μM<sup>-1</sup> h<sup>-1</sup> (the most reliable<sup>7</sup> value is 0.43 μM<sup>-1</sup> h<sup>-1</sup>). The inactivation rate constants are discussed in the results.

It is instructive to note the conditions under which these mechanisms reduce to familiar limiting cases (Scheme 1). If the kinetic intermediate in eqs 4 and 5 is very short-lived (*i.e.*  $k_r \gg k_{on}[P^*]$  and  $k_{off} \gg k_e$ ), the kinetic intermediate mechanism simplifies to that described by eqs 1–3. In the case where  $k_{on}[P^*] \gg k_i$ , this simpler mechanism resembles a

### Scheme 1. Simplified Mechanisms for Limiting Cases



two-step consecutive reaction for which analytical solutions are available.<sup>14</sup> In addition, if the dissociation of endogenous peptide is not rate limiting (*i.e.*  $k_e \gg k_{on}[P^*] \gg k_i$ ), the reaction resembles a simple reversible association process. If dissociation of the endogenous peptides and added labeled peptide are very fast, the binding reaction rapidly equilibrates relative to protein inactivation. An analytical solution to eqs 6–9 derived under these conditions has been used to estimate  $K_d$  and  $k_i$  for short-lived MHC protein–peptide complexes.<sup>7</sup> This derivation can also be extended to a mechanism that includes a kinetic intermediate.<sup>7,15</sup>

Experimentally, a very large excess of labeled peptide (~100-fold) is typically required to attain binding saturation. Under these circumstances rebinding of  $P_e$  by reaction 1 must generally be negligible. However, in the simulations, saturation is attained at lower  $P^*$  concentrations (~10-fold excess). Since rebinding of  $P_e$  is not judged to be significant in the experiments, this rebinding is omitted in the simulations. The simulations do not take into account the peptide activity, which may be reduced sometimes by detergent binding and aggregation. We suspect it is for this reason that saturation is found at ~10-fold excess peptide in the simulations, but only ~100-fold excess in some experiments.

### Results and Discussion

**Small Inactivation Rates—The Limiting Case.** The reactions of MHC proteins with peptides were simulated so as to

(14) Fersht, A. *Enzyme Structure and Mechanism*; W. H. Freeman and Co.: New York, 1985; pp 139–141.

(15) In ref 7 it was shown that rapid equilibration of binding relative to inactivation allows for the simplified expression  $mP^*(t) = C(e^{-kt} - e^{-k_e t})$  where  $C = (k_e [mP_e]_0 [P^*]) / (k_e - k)(K_d + [P^*])$  and  $k = k_i K_d / (K_d + [P^*])$ . If this rapidly formed complex is thought of as an intermediate that subsequently forms a very long-lived complex, as in eq 6, then this same solution is valid with  $k = (k_i K_d + k_r [P^*]) / (K_d + [P^*])$ .

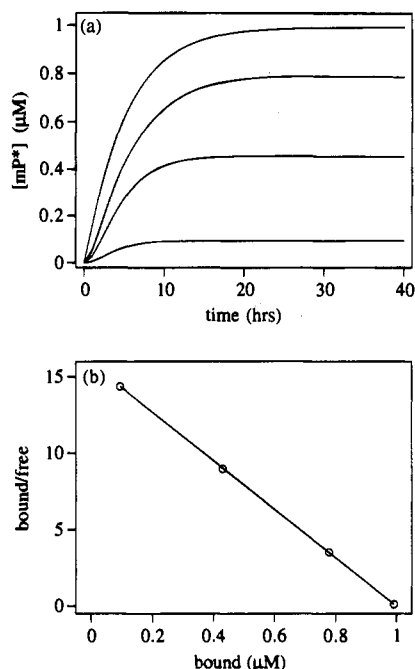


**Figure 1.** (a) Simulated binding curves for the mechanism described by eqs 1–3 at different peptide concentrations and (b) a plot of the Scatchard analysis of the binding curves in (a). The rate constants used for the simulation were as follows:  $k_e = 0.2 \text{ h}^{-1}$ ,  $k_{on} = 0.72 \mu\text{M}^{-1} \text{ h}^{-1}$ ,  $k_{off} = 0.03 \text{ h}^{-1}$ ,  $k_i = 0.1 \text{ h}^{-1}$ ,  $K_d = 42 \text{ nM}$ . The protein concentration was  $1.0 \mu\text{M}$  and the peptide concentrations were 0.1, 0.5, 1.0, and  $10 \mu\text{M}$ . The slope of (b) gives an apparent  $K_d = 63 \text{ nM}$  and the X-intercept is  $1.0 \mu\text{M}$ .

**Table 1.** Representative Rate Constants Used in Simulations of the Mechanism Described by Eqs 1–3

$k_e (\text{h}^{-1})$	0.2	0.04	0.05
$k_{on} (\mu\text{M}^{-1} \text{h}^{-1})$	0.4	1.0	0.4
$k_{off} (\text{h}^{-1})$	0.08	0.03	0.001
$k_i (\text{h}^{-1})$	0.001	0.001	0.1
$K_d (\text{nM})$	200	30	2.5
apparent $K_d (\text{nM})^a$	470	160	260

<sup>a</sup> Derived from the corresponding Scatchard plots.

reproduce the range of observed kinetic rates. Representative simulated binding curves for the mechanism described by eqs 1–3 are illustrated in Figure 1a. A “Scatchard analysis” of these binding curves can be made using the long time limit of the amount of peptide bound, when this is approximately constant. An analysis of this type gives a linear plot (Figure 1b) with an intercept that corresponds to one binding site and a slope that gives an apparent  $K_d$  of 62 nM. The  $K_d$  used in the simulation is 42 nM. Simulations over a wide range of each of the rate constants yielded binding curves for which the Scatchard plots were frequently linear ( $R > 0.9990$ ). There is no simple relationship between the  $K_d$  values used in the simulations and those determined from the corresponding Scatchard plots; the two values often differ by as much as 100-fold (Table 1). Of course, as the inactivation rate constant  $k_i$  is decreased, the slopes of the Scatchard plots approach the equilibrium constants. For example, if the reactions in Figure 1a are simulated with a  $k_i$  of  $0.001 \text{ h}^{-1}$ , the corresponding Scatchard plot gives a  $K_d$  of 43 nM. However, in the case where this inactivation rate has been measured it is of the order of  $0.3 \text{ h}^{-1}$ .<sup>7</sup>

Representative simulated binding curves for a mechanism that includes a kinetic intermediate, eqs 4 and 5, are illustrated in Figure 2a. The rate constants used in these simulations were derived from the kinetics of the reactions of the sperm whale myoglobin 110–121 peptide with the MHC protein I-E<sup>d</sup>.<sup>5,16</sup> The

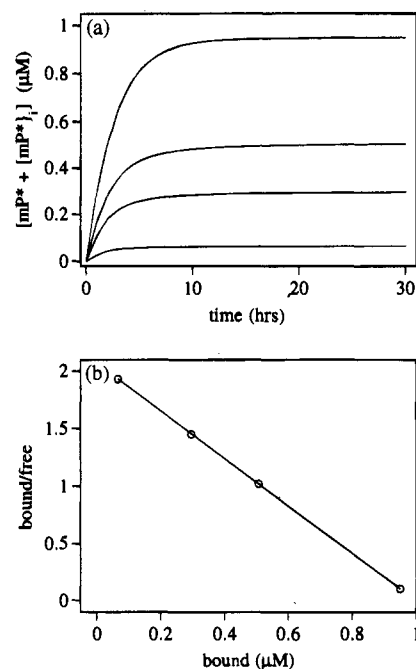


**Figure 2.** (a) Simulated binding curves for the mechanism that includes a kinetic intermediate, eqs 4 and 5, at different peptide concentrations and (b) a plot of the Scatchard analysis of the binding curves in (a). The rate constants used for the simulation were as follows:  $k_e = 0.4 \text{ h}^{-1}$ ,  $k_{on} = 5.0 \mu\text{M}^{-1} \text{ h}^{-1}$ ,  $k_{off} = 3.0 \text{ h}^{-1}$ ,  $k_f = 0.025 \text{ h}^{-1}$ ,  $k_r = 0.08 \text{ h}^{-1}$ ,  $k_i = 0.001 \text{ h}^{-1}$ ,  $k_{off}/k_{on} = 0.60 \mu\text{M}$ . The protein concentration was  $1.0 \mu\text{M}$  and the peptide concentrations were 0.1, 0.5, 1.0, and  $10 \mu\text{M}$ . The slope of (b) gives an apparent  $K_d = 0.48 \mu\text{M}$  and the X-intercept is  $1.0 \mu\text{M}$ .

**Table 2.** Representative Rate Constants Used in Simulations of the Mechanism That Includes a Kinetic Intermediate<sup>a</sup>

$k_e (\text{h}^{-1})$	0.4	0.05	0.2
$k_{on} (\mu\text{M}^{-1} \text{h}^{-1})$	1.0	3.0	30
$k_{off} (\text{h}^{-1})$	3.0	3.0	3.0
$k_f (\text{h}^{-1})$	0.05	0.03	0.03
$k_r (\text{h}^{-1})$	0.005	0.02	0.02
$k_i (\text{h}^{-1})$	0.01	0.005	0.005
$k_{off}/k_{on} (\mu\text{M})^b$	3.0	1.0	0.1
apparent $K_d (\mu\text{M})^c$	0.68	0.61	0.057

<sup>a</sup> As described by eqs 4 and 5. <sup>b</sup>  $K_d$  for reaction 4. <sup>c</sup> Derived from the corresponding Scatchard plots.

ratio  $k_{off}/k_{on} = 0.60 \mu\text{M}$ ,  $K_d$  for reaction 4, was used in the simulations for Figure 2a and the slope of the corresponding Scatchard plot (Figure 2b) gives an apparent  $K_d$  of  $0.48 \mu\text{M}$ . Despite this increased kinetic complexity, the Scatchard plots are frequently linear and the apparent  $K_d$  values differ from the equilibrium constants for reaction 4 by less than 10-fold (Table 2). If the intermediate and terminal complexes are short- and long-lived, respectively, the relative amount of MHC protein partitioned between the binding and inactivation reactions is proportional to the stability of the intermediate complex. Thus, the slope of a corresponding Scatchard plot for mechanism 4–5 is anticipated to be more closely related to the equilibrium constant for the kinetic intermediate.<sup>17</sup> Simulations in which the intermediates are long-lived are qualitatively equivalent to simulations of the simpler mechanism described by eqs 1–3.

(16) Some of the rate constants used for this simulation (Figure 3 legend) differ from those reported in ref 5. The previously reported simulations of these reactions included a step for rebinding of the endogenous peptides which has been eliminated (see Experimental Section). The inactivation and association rate constants used for Figure 3 are lower than in ref 5. However, the simulations illustrated in Figure 3 accurately reproduce all the experimentally reported<sup>5</sup> features of the reactions of the myoglobin 110–121 peptide and I-E<sup>d</sup>.

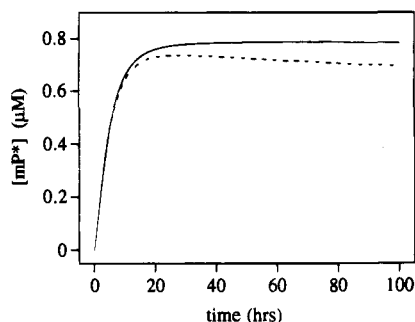


**Figure 3.** Simulated binding curves for the mechanism described by eqs 1–3 with an endogenous peptide population characterized by one (broken line) and two (solid line) dissociation rates. For the single dissociation rate,  $k_e = 0.1 \text{ h}^{-1}$  and  $[mP_e]_0 = 0.8 \text{ } \mu\text{M}$ . For the double dissociation rate,  $k_e = 0.2$  and  $0.01 \text{ h}^{-1}$  with initial concentrations of 0.8 and  $0.2 \text{ } \mu\text{M}$ , respectively. For both simulations the added peptide concentration was  $1.0 \text{ } \mu\text{M}$  and  $k_{on} = 3.6 \text{ } \mu\text{M}^{-1} \text{ h}^{-1}$ ,  $k_{off} = 0.01 \text{ h}^{-1}$ ,  $k_i = 0.1 \text{ h}^{-1}$ .

**Estimated Inactivation Rate Constants.** The inactivation rate constant for the MHC protein I-A<sup>k</sup>, determined from a kinetic analysis, is  $k_i = 0.32 \text{ h}^{-1}$  at  $37 \text{ } ^\circ\text{C}$ .<sup>7</sup> The MHC protein I-E<sup>d</sup> is inactivated with an observed rate of  $0.043 \text{ h}^{-1}$  when incubated at  $37 \text{ } ^\circ\text{C}$  in the absence of added peptide.<sup>5</sup> This latter apparent rate is potentially affected by the loss of endogenous peptides. However, the reactions of the sperm whale myoglobin 110–121 peptide with I-E<sup>d</sup> can be simulated with an endogenous peptide dissociation rate  $k_e = 0.40 \text{ h}^{-1}$  (Figure 2a). Thus, we infer that the observed inactivation rate for I-E<sup>d</sup> corresponds to the rate constant  $k_i$ .

The MHC protein DR1 produced by baculovirus expression in insect cells is free of peptide and, thus, the binding of added peptide does not depend on the prior dissociation of endogenous peptide.<sup>4,9</sup> It has been shown that about 80% of the insect cell DR1 protein is inactivated when incubated at  $37 \text{ } ^\circ\text{C}$  for 31 h without peptide; this corresponds to an inactivation rate constant of  $k_i = 0.05 \text{ h}^{-1}$ .<sup>4b</sup> Thus, realistic simulations of the reactions of the MHC proteins require inactivation rate constants that encompass the range  $k_i = 0.01\text{--}1.0 \text{ h}^{-1}$ .

In most cases, binding curves simulated with the higher inactivation rate constants ( $k_i = 0.01\text{--}1.0 \text{ h}^{-1}$ ) do not attain the observed stable plateaus (Figure 3, broken line) unless the peptide dissociation rate constant,  $k_{off}$ , is extremely small ( $k_{off} \leq 0.001 \text{ h}^{-1}$ ). This instability is reduced if heterogeneity of endogenous peptides is included in the reaction kinetics.<sup>10</sup> Very slow dissociation of some population of endogenous peptides bound to the MHC proteins compensates for the decreased binding (Figure 3) caused by protein inactivation. Thus, the rate of dissociation of endogenous peptides is best simulated as an ensemble of dissociation reactions. Unfortunately, the dissociation rate constants for endogenous peptides are not known. Dissociation rate constants for antigenic peptides cover a large range. For example, rate constants for the dissociation of antigenic peptides from the MHC protein I-A<sup>k</sup> are in the range  $k_{off} = 1\text{--}0.001 \text{ h}^{-1}$ .<sup>7</sup>

Heterogeneity in chemical reaction rates can be represented with a power function of the form  $f(t) = f_0(1 + t/t_0)^{-n}$ , which describes an ensemble of rate constants distributed about  $n/t_0$ ,

(17) If it is assumed that the terminal complex does not revert to the intermediate ( $k_r \sim 0$ ), the equilibrium dissociation constant also corresponds to the peptide concentration at which half of the protein is inactivated and half forms the terminal complex. As the intermediate conversion or inactivation rates ( $k_f$  and  $k_i$ , respectively) approach the dissociation rate  $k_{off}$ , or if the terminal complex reverts to intermediate, the slopes of the Scatchard plots begin to deviate from the equilibrium constant for reaction 4.

the most probable rate constant.<sup>18</sup> However, the use of this power function to describe the dissociation of endogenous peptides does not produce binding curves consistent with experimental observations.<sup>19</sup> We found that realistic kinetic binding curves are generated from simulations in which the dissociation of endogenous peptides is described by two rate constants (Figure 3, solid line). This is consistent with the observation that distributions of dissociation rate constants for antigenic peptides are approximately bimodal.<sup>20</sup>

The reactions of the hen egg white lysozyme (46–61) and myelin basic protein Ac(1–14)-A<sup>4</sup> peptides with the MHC protein I-A<sup>k</sup> differ significantly. The lysozyme peptide binds I-A<sup>k</sup> slowly (80–100 h) and dissociates with  $k_{off} = 0.001 \text{ h}^{-1}$ . In contrast, the amount of complex formed between I-A<sup>k</sup> and the myelin peptide attains a maximum within several hours and then rapidly decreases; the peptide dissociates with  $k_{off} = 1.2 \text{ h}^{-1}$ .<sup>7</sup> These two reactions were simulated with the mechanism described by eqs 1–3 using a bimodal distribution of endogenous peptides and experimentally determined rate constants.<sup>7</sup> The simulated binding curves show an excellent correspondence with experimental data for these reactions (Figure 4). We emphasize that the only parameter that differs between the two simulations is the peptide dissociation rate constant  $k_{off}$ . Reactions of the lysozyme peptide with I-A<sup>k</sup> simulated at different peptide concentrations were also analyzed with a Scatchard plot (Figure 5). The  $K_d$  used in the simulations was  $2.8 \text{ nM}$  while the slope of the Scatchard plot gave an apparent  $K_d = 0.52 \text{ } \mu\text{M}$ . The reported  $K_d$  value for this complex, determined by Scatchard analysis, is  $2.0 \text{ } \mu\text{M}$ .<sup>22</sup>

Reactions of peptides with the MHC proteins were also simulated with the mechanism that includes a kinetic intermediate, eqs 4 and 5, using bimodal distributions of the endogenous peptides and the higher inactivation rate constants ( $k_i = 0.01\text{--}1.0 \text{ h}^{-1}$ ). As observed with the smaller inactivation rates, the corresponding Scatchard plots are frequently linear with slopes that differ from the equilibrium constants for the intermediate by less than 10-fold. At these higher inactivation rates, Scatchard plots for simulations of both mechanisms are often slightly nonlinear (*i.e.* see Figure 5). It is unlikely that such small curvatures would be discerned experimentally. The Scatchard plots of binding curves simulated with even larger inactivation rates ( $k_i > 1.0 \text{ h}^{-1}$ ) are often highly nonlinear ( $R < 0.98$ ). Since experimentally determined Scatchard plots are linear, we suggest that a  $k_i$  value of  $1.0 \text{ h}^{-1}$  is probably an upper limit.<sup>23</sup>

(18) Austin, R. H.; Beeson, K.; Eisenstein, L.; Frauenfelder, H.; Gunsulas, I. C.; Marshall, V. P. *Phys. Rev. Lett.* **1974**, *32*, 403–405.

(19) Descriptions of the dissociation of endogenous peptides with these power functions produce simulated binding curves in which the initial slopes are too small. To obtain steeper initial slopes, the distribution of dissociation rates must be highly compressed about a relatively high most probable rate which produces curves similar to those generated with a single dissociation rate (*i.e.* Figure 3, dotted line).

(20) Typically, dissociation rates are small ( $k_{off} < 0.02 \text{ h}^{-1}$ ).<sup>3–9</sup> There have also been a few reports of peptides that dissociate rapidly ( $k_{off} = 1\text{--}3 \text{ h}^{-1}$ ).<sup>5–7,22</sup> The MHC protein I-E<sup>k</sup>, an  $\alpha\beta$  heterodimer, dissociates into  $\alpha$  and  $\beta$  chains when incubated at  $37 \text{ } ^\circ\text{C}$  in octyl glucoside without peptide.<sup>6</sup> The kinetics of this cleavage reaction are biphasic with rate constants 0.1 and  $0.006 \text{ h}^{-1}$ .<sup>6</sup> It is likely that some of the endogenous peptides bound to I-E<sup>k</sup> dissociate quickly and that the fast phase,  $k = 0.1 \text{ h}^{-1}$ , is the intrinsic heterodimer cleavage rate under these conditions. Slow dissociation of another population of endogenous peptides would be rate limiting and correspond to  $k_e = 0.006 \text{ h}^{-1}$ .

(21) Fairchild, P. J.; Wildgoose, R.; Atherton, E.; Webb, S.; Wraith, D. *C. Int. Immunol.* **1993**, *5*, 1151–1158.

(22) Babbit, B. P.; Allen, P. A.; Matsueda, G.; Haber, E.; Unanue, E. R. *Nature (London)* **1985**, *317*, 359–361.

(23) In addition, we suggest that the inactivation of MHC protein is unimolecular since Scatchard plots of simulations with a bimolecular (second order) inactivation reaction are highly nonlinear ( $R < 0.7$ ).

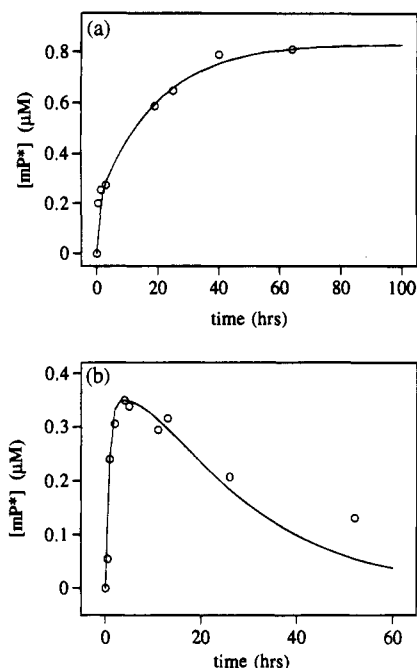


**Figure 4.** Simulated binding curves (solid line) and experimental data (○) for the reactions of (a) the hen egg white lysozyme 46–61 peptide and (b) the myelin basic protein Ac(1–14) A<sup>4</sup> peptide with the murine class II MHC protein I-A<sup>k</sup>. The binding curves are simulations of the mechanism described by eqs 1–3 with two dissociation rates for the endogenous peptides. The protein intensive rate constants used were  $k_{e1} = 2 \text{ h}^{-1}$ ,  $k_{e2} = 0.05 \text{ h}^{-1}$ ,  $[\text{mP}_{e1}] = 0.2 \text{ } \mu\text{M}$ ,  $[\text{mP}_{e2}] = 0.8 \text{ } \mu\text{M}$ , and  $k_i = 0.3 \text{ h}^{-1}$ . Both peptides were simulated at a concentration of  $5.0 \text{ } \mu\text{M}$  with  $k_{on} = 0.36 \text{ } \mu\text{M}^{-1} \text{ h}^{-1}$ . The dissociation rates ( $k_{off}$ ) for the hen egg white lysozyme 46–61 (a) and myelin basic protein Ac(1–14) A<sup>4</sup> (b) peptides were 0.001 and  $1.2 \text{ h}^{-1}$ , respectively. Experimental data for (b) was taken from ref 7; data for (a) was acquired as described in ref 18.

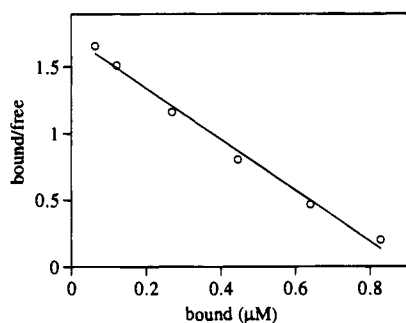


**Figure 5.** A Scatchard plot for a set of simulated binding curves for the reactions of the hen egg white lysozyme 46–61 peptide with the murine class II MHC protein I-A<sup>k</sup> as described for Figure 4. The rate constants used in the simulations are given in the Figure 4 legend and the peptide concentrations ranged from  $0.1$  to  $10 \text{ } \mu\text{M}$ . The  $K_d$  used in the simulation was  $2.8 \text{ nM}$  and the apparent  $K_d$  determined from the slope of the Scatchard analysis is  $0.52 \text{ } \mu\text{M}$ . The correlation coefficient for the linear fit in the Scatchard plot is  $R = 0.9958$ .

**Simulations of Inhibition Assays.** Relative peptide affinities for MHC proteins (*i.e.* equilibrium constants) are often inferred from inhibition assays in which the binding of a well-characterized peptide is competed by a second peptide. Inhibition assays were simulated with the mechanism described by eqs 1–3 using a bimodal distribution of endogenous peptides; a representative  $\text{IC}_{50}$  plot is shown in Figure 6. Although the relative order of inhibitor peptide  $\text{IC}_{50}$  values obtained from the plot is correct, the  $\text{IC}_{50}$  values are not quantitatively related

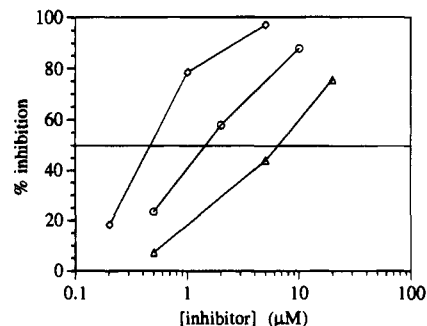


**Figure 6.** Simulated inhibition of peptide binding assays. Competition reactions were simulated with the mechanism described by eqs 1–3 and two dissociation rates for the endogenous peptides. The protein intensive rate constants used were  $k_{e1} = 0.2 \text{ h}^{-1}$ ,  $k_{e2} = 0.01 \text{ h}^{-1}$ ,  $[\text{mP}_{e1}] = 0.8 \text{ } \mu\text{M}$ ,  $[\text{mP}_{e2}] = 0.2 \text{ } \mu\text{M}$ , and  $k_i = 0.01 \text{ h}^{-1}$ . The peptide whose binding was being competed had a concentration of  $1.0 \text{ } \mu\text{M}$  with  $k_{on} = 0.36 \text{ } \mu\text{M}^{-1} \text{ h}^{-1}$  and  $k_{off} = 0.03 \text{ h}^{-1}$  ( $K_d = 83 \text{ nM}$ ). The three peptides used to inhibit binding had rate constants of ( $\diamond$ )  $k_{on} = 3.6 \text{ } \mu\text{M}^{-1} \text{ h}^{-1}$  and  $k_{off} = 0.03 \text{ h}^{-1}$ , ( $\circ$ )  $k_{on} = 0.36 \text{ } \mu\text{M}^{-1} \text{ h}^{-1}$  and  $k_{off} = 0.03 \text{ h}^{-1}$ , and ( $\triangle$ )  $k_{on} = 0.36 \text{ } \mu\text{M}^{-1} \text{ h}^{-1}$  and  $k_{off} = 0.3 \text{ h}^{-1}$ . Percent of binding inhibition (no competitor) was calculated at inhibitor peptide concentrations ranging from  $0.2$  to  $20 \text{ } \mu\text{M}$ . The inhibitor peptide  $K_d$  (simulated) and  $\text{IC}_{50}$  (extrapolated) values are ( $\diamond$ )  $K_d = 8.3 \text{ nM}$ ,  $\text{IC}_{50} = 0.46 \text{ } \mu\text{M}$ , ( $\circ$ )  $K_d = 83 \text{ nM}$ ,  $\text{IC}_{50} = 1.4 \text{ } \mu\text{M}$ , and ( $\triangle$ )  $K_d = 0.83 \text{ } \mu\text{M}$ ,  $\text{IC}_{50} = 5.6 \text{ } \mu\text{M}$ .

to the peptide affinities. For example, in the simulations represented in Figure 6, the inhibitor-peptide affinities differ by 100-fold ( $K_i = 8.3 \text{ nM}$  to  $0.83 \text{ } \mu\text{M}$ ) while the extrapolated  $\text{IC}_{50}$  values differ by slightly more than 10-fold ( $0.46$ – $5.6 \text{ } \mu\text{M}$ ). The ratios of  $\text{IC}_{50}$  and  $K_i$  values should be equal for simple competitive inhibition. In addition, a Schild analysis<sup>24</sup> of competition reactions simulated with an inhibitor peptide  $K_i = 83 \text{ nM}$  gave a linear plot ( $R = 0.997$ ) with a slope of 1.1 (simple competitive inhibition) and an intercept that corresponded to a  $K_i$  of  $4.6 \text{ } \mu\text{M}$ . Interpretations of these inhibition assays are also compromised by inactivation of the MHC protein.

**Concluding Remarks.** Inactivation of an MHC protein during its reactions with peptides was first reported in 1992.<sup>6</sup> More recent demonstrations of protein inactivation with murine<sup>5,7</sup> and human<sup>4b</sup> class II MHC proteins points to the generality of this inactivation reaction. We have found that Scatchard plots of reactions simulated with protein inactivation included are frequently linear, as observed experimentally. Inclusion of reasonable estimates for the inactivation rate constants in simulations of these reactions suggests that the distribution of dissociation rates for the endogenous peptides is at least bimodal. The inclusion of these features in mechanistic simulations enables us to reproduce accurately markedly different reactions of the MHC protein I-A<sup>k</sup>. The apparent  $K_d$  derived from the Scatchard plot of one of these simulations is also remarkably similar to the experimentally reported value but is three orders of magnitude different from the  $K_d$  used in the simulations. Thus, the apparent  $K_d$  values derived from Scatchard plots for these reactions have no clear significance.

**Acknowledgment.** This work was supported by National Institutes of Health Grant No. 5R37 AI13587-17. C.B. gratefully acknowledges financial support from the Cancer Research Institute.

JA951327G